NiO spacer mediated magnetic anisotropy in $L1_0$-FePt/NiO/$A1$-FePt trilayer structures

Tenghua Gao,[1,2] Takashi Harumoto,[1] Song Zhang,[2] Rong Tu,[2] Lianmeng Zhang,[2] Yoshio Nakamura,[1] and Ji Shi[1,*]

[1]*School of Materials and Chemical Technology, Tokyo Institute of Technology, 2-12-1 Oh-okayama, Meguro-ku, Tokyo 152-8552, Japan*

[2]*State Key Laboratory of Advanced Technology for Materials Synthesis and Processing, Wuhan University of Technology, 122 Luoshi Road, Wuhan 430074, People's Republic of China*

(Received 20 January 2017; revised manuscript received 8 March 2017; published 4 April 2017)

$L1_0$-FePt/NiO/$A1$-FePt trilayers have been grown on MgO(001) substrate, in which the top FePt layer is of $A1$ structure, and the bottom FePt layer is of $L1_0$ structure with 001 preferred orientation and strong perpendicular anisotropy. This structure gives rise to a 90° spin alignment configuration of the two ferromagnetic layers across the NiO spacer. To further manipulate the spin configurations of the trilayer structure, we performed an in-plane field cooling (FC). The subsequent hysteresis measurements for the top FePt layer show unambiguous angular dependence of remanent magnetization relative to the direction of the field during FC; i.e., in-plane anisotropy is induced. Taking into account the spin-flop configuration predicted in previous theoretical study, the coupling at the lower interface makes the Ni spins cant out of the $(\bar{1}\,\bar{1}\,1)$ easy plane, and difficult to rotate around the axis perpendicular to the film plane. Correspondingly, the induced anisotropy after FC is considered to result from the realignment of Ni spins and enhancement of the coupling at the upper interface. The magnetic domain imaging results for the bottom perpendicular magnetized FePt layer strongly support this consideration; some of the stripe domains tend to be along the direction of the applied field during FC with reduced stripe width.

DOI: 10.1103/PhysRevB.95.134406

I. INTRODUCTION

The exchange bias effect [1] originating from interfacial coupling between ferromagnetic (FM) and antiferromagnetic (AFM) layers appears to play an important role in zero-field spin-orbit torque (SOT) induced magnetization switching in modern spintronics technology [2,3]. Although several models have been developed to explain this effect [4–8], the complexity of the FM/AFM interface in the real case makes it difficult to present a general theory for FM-AFM interfacial interaction. Recently, it was experimentally proven that the FM and AFM spins can be coupled orthogonally at the compensated AFM interface, for instance, Fe/NiO(001) [9,10] or Fe/CoO(001) [11,12] coupled structures. However, due to the absence of induced unidirectional anisotropy, a new pinning mechanism for exchange bias in such orthogonal coupling structures must be proposed rather than Mauri's model [10]. In order to address this issue, a detailed study on the FM-AFM coupling configuration at the compensated AFM interface is highly required.

Realizing that at the FM/AFM interface the AFM order can induce various types of magnetic anisotropy [13], or even change the perpendicular magnetic anisotropy in the adjacent FM layer [14], an alternative approach to investigate the FM-AFM coupling configuration is to study how the FM layer responds to the change of AFM order inside the AFM layer. It was found recently that in Py/FeMn/Ni trilayers [15], the in-plane magnetization of Ni enhances the Py fourfold anisotropy. The authors speculated that the reason for this enhancement is a slight increase of the FeMn spin in-plane component caused by direct coupling between Ni and FeMn spins. This result indicates that in such trilayer structure the weak anisotropy of the FM layer makes it sensitive to the modification of the AFM spin structure, which offers an opportunity to make detailed indirect observation on the FM-AFM coupling configuration. On the other hand, the study of interlayer exchange coupling (IEC) of two FM layers across a non-FM insulating spacer has been stimulated since the discovery of tunneling magnetoresistance [16]. Among insulating spacer based structures, it is of particular interest for the case of FM layers separated by an antiferromagnetic insulating spacer due to its unexpected behavior [17]. For the NiO spacer, the occurrence of a 90° in-plane IEC has been observed in Fe_3O_4/NiO/Fe_3O_4 [18], $Ni_{80}Fe_{20}$/NiO/Co [19], and Co/NiO/Fe structures [20]. This anomalous interlayer coupling was explained by contradictory mechanisms, either the formation of 90° spiraling spin structure in the AFM spacer going from one FM/AFM interface to the other [18], or the collinear and orthogonal FM-AFM coupling separately presented at two FM/AFM interfaces [19] resulting from the interface roughness. The key point of all these works is to puzzle out the 90° IEC mechanisms. Moreover, it is well accepted that field cooling (FC) could lead to the repopulation of AFM magnetic domains [21], and the realignment of the AFM spins depends on the local FM order [22,23]. Recalling the various results and points of view described above, we think it is interesting to propose a trilayer structure, in which regardless of the NiO spacer, the spins between two FM layers are "naturally" aligned as a 90° configuration. Through a certain FC treatment to realign the AFM spins in the NiO spacer, it should be possible to study whether the modification of AFM spin structure can influence the magnetic behavior of adjacent FM layers.

In this paper, we present an investigation of the $L1_0$-FePt/NiO/$A1$-FePt trilayer structure, in which the top FePt layer is of the $A1$ structure, and the bottom FePt layer is of the $L1_0$ structure with 001 preferred orientation and strong perpendicular magnetic anisotropy. The fascinating feature of this structure is that the strong perpendicular magnetic anisotropy of the bottom layer and magnetic dipolar anisotropy of the top layer give rise to a 90° spin alignment configuration of the two FM layers across the NiO spacer, while the in-plane

*Corresponding author: shi.j.aa@m.titech.ac.jp

magnetic anisotropy of top FePt layer can be hardly influenced by the bottom one. Through an in-plane FC with 500 Oe external fields to realign the Ni spins, we find that in-plane magnetic anisotropy in the $A1$-disordered top FePt layer and the magnetic stripe domain structure in the $L1_0$-ordered bottom FePt layer were significantly changed. Based on our experimental results, the configuration of FM-AFM interfacial coupling has been carefully discussed.

II. EXPERIMENTAL

Reference $FePt_{Oop}$(4.5 nm)/NiO(4 nm) bilayers (S1) and $FePt_{Oop}$(4.5 nm)/NiO(t nm)/$FePt_{Ip}$(3.5 nm) trilayers were sputtered on a single-crystal MgO(001) substrate. Here, the subscripts Oop and Ip refer to the out-of-plane and in-plane magnetization, respectively, and t refers to the thickness of the NiO layer. The preparation conditions for bilayers have been described in our previous work [24], and the only difference is that in order to trigger the $L1_0$ phase transformation (perpendicular magnetic anisotropy) for relatively thicker FePt layer, an elevated substrate temperature of 723 K was used. For trilayer structure, a FePt(3.5 nm) layer was subsequently deposited on the top of the bilayers at 373 K. With this substrate temperature the top FePt layer remains disordered and the Fe magnetization of the FePt layer is in the film plane. The thicknesses of the NiO layer were chosen as 2 (S2) and 4 nm (S3). Finally, the trilayer samples were capped by 2 nm of NiO sputtered at room temperature (RT). An additional sample of $FePt_{Ip}$(3.5 nm)/NiO(4 nm)/$FePt_{Ip}$(3.5 nm) (S4) was also prepared. In this trilayer structure, the two FePt layers were grown under the same conditions as the top disordered FePt layer in samples of S2 and S3. Besides that, other preparation conditions were the same as samples of S2 and S3. The FePt/NiO/FePt trilayer structures grown on the MgO(001) single-crystal substrate give rise to an extraordinary crystallographic relationship among the layers. The structure of the sample was characterized by x-ray diffraction (XRD). To understand the influence of the FM-AFM coupling configuration on two FM layers, the samples were cooled through Néel temperature ($T_N \sim 523$ K) in a low vacuum (1.33 Pa) by using two different FC treatments: (i) an in-plane FC with 500 Oe external fields along the MgO [100] axis to saturate the $A1$-disordered FePt layer; (ii) an out-of-plane FC in 8 kOe fields to align the magnetization of the $L1_0$-ordered FePt layer along the film normal direction. The magnetic properties were measured by a vibrating sample magnetometer (VSM) at RT and the flexible sample holder allows measurements conducted along different in-plane directions. The room temperature magnetic domain imaging was performed by magnetic force microscopy (MFM).

III. RESULTS AND DISCUSSION

A. Establishment of 90° spin alignment configuration of the two FM layers across the NiO spacer

Figure 1 shows the hysteresis loops recorded at RT for samples S1, S3, and S4, and the magnetic fields were applied perpendicular to the film surface. It is seen that the $FePt_{Oop}$/NiO bilayers exhibit a sharp square loop with 1.46 kOe coercive field as shown in Fig. 1(c) (black loop),

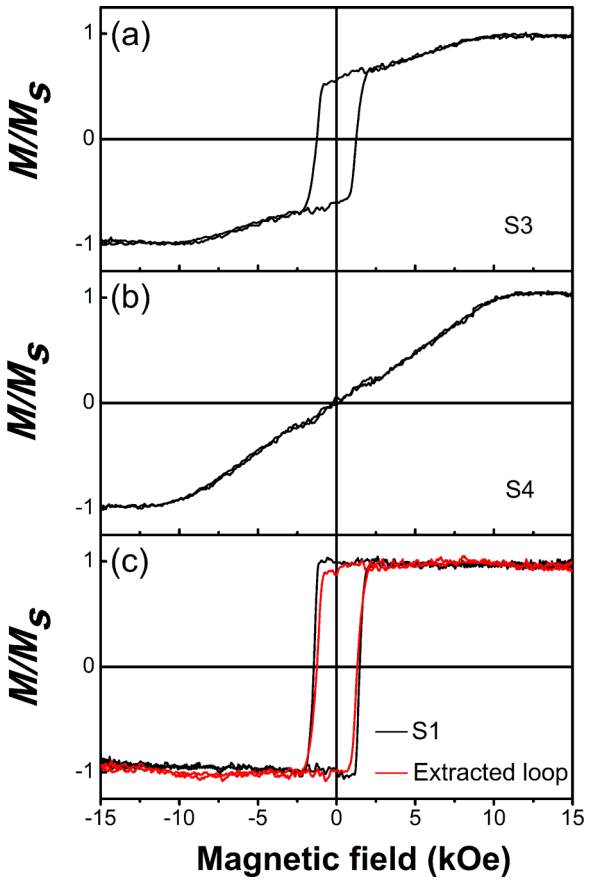

FIG. 1. Hysteresis loops along the film normal direction for (a) $FePt_{Oop}$(4.5 nm)/NiO(4 nm)/$FePt_{Ip}$(3.5 nm) (S3), and (b) $FePt_{Ip}$(3.5 nm)/NiO(4 nm)/$FePt_{Ip}$(3.5 nm) (S4) trilayers. (c) Perpendicular hysteresis loop of extracted FePt bottom layer (red loop) and that of $FePt_{Oop}$(4.5 nm)/NiO(4 nm) bilayers (S1) (black loop). The extracted loop was obtained from samples of S3 and S4, through the following relationship: $M_{\text{bottom}} = M_{S3} - M_{S4}/2$.

while for $FePt_{Ip}$/NiO/$FePt_{Ip}$ trilayers, along the same direction a remanent magnetization of almost 0% is observed in Fig. 1(b). In the case of the $FePt_{Oop}$/NiO/$FePt_{Ip}$ trilayer structure as shown in Fig. 1(a), the remanent magnetization is 57% and it is apparent that magnetization rotation occurred before saturation, which can be understood as the magnetizations of the top and bottom FePt layers being oriented perpendicular to each other. These results confirm that in $FePt_{Oop}$/NiO/$FePt_{Ip}$ trilayer structure, owing to the strong perpendicular magnetic anisotropy in the $L1_0$-ordered FePt and the magnetic dipolar anisotropy in the $A1$-disordered FePt, the magnetization of the bottom and top FePt layers are restrained along the film normal and in-plane directions, respectively. Assuming no direct coupling between the two FePt layers, through subtracting the contribution of the $A1$-disordered FePt layer [data of Fig. 1(b)], from Fig. 1(a) the perpendicular hysteresis loop for the bottom FePt layer should remain as shown in Fig. 1(c) (red loop). Compared with the loop of $FePt_{Oop}$/NiO bilayers, the similar square shape for the extracted loop confirms that the two FM layers in the $FePt_{Oop}$/NiO/$FePt_{Ip}$ trilayer structure exhibit a 90° spin configuration. On account of the differences, a slight decrease of the coercive field can be observed in the

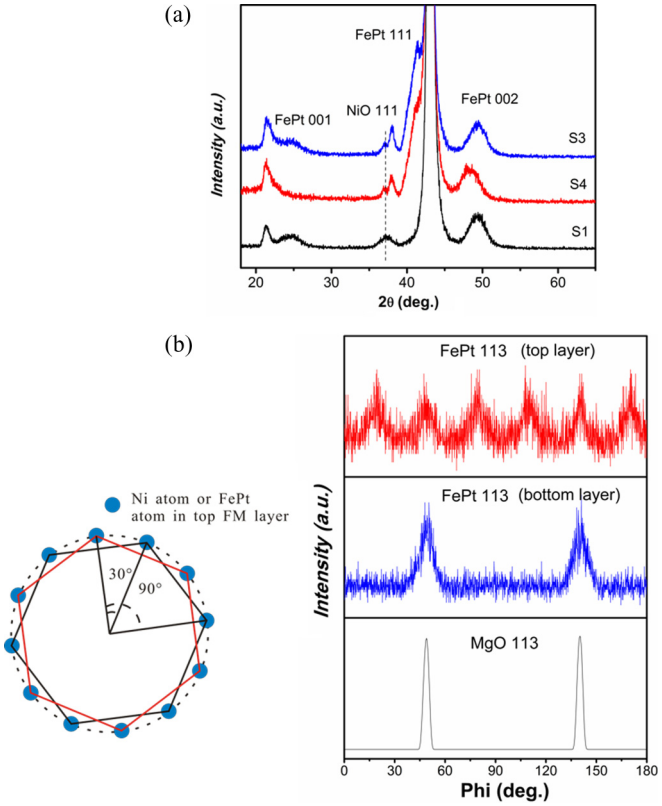

FIG. 2. (a) The XRD θ-2θ scans of $FePt_{Oop}$(4.5 nm)/NiO (4 nm) bilayers (S1) (black pattern), $FePt_{Oop}$(4.5 nm)/NiO(4 nm)/$FePt_{Ip}$(3.5 nm) trilayers (S3) (blue pattern), and $FePt_{Ip}$(3.5 nm)/NiO(4 nm)/$FePt_{Ip}$(3.5 nm) (S4) (red pattern). (b) XRD 180° φ-scan plot for $FePt_{Oop}$(4.5 nm)/NiO(4 nm)/$FePt_{Ip}$(3.5 nm) (S3) trilayer structure. The inset shows the schematic illustration of the in-plane atomic arrangement of NiO and top FePt layer.

extracted loop, which is considered to result from the magnetic anisotropy of the FM layer mediated by the NiO spacer and mainly related to the FM-AFM coupling configuration.

It is well known that, for NiO, the FM-AFM coupling configuration is dominated by the magnetoelastic effect resulting from epitaxial strain [9,25], and is strongly related to the epitaxial relationship. Thus, to discuss the spin configuration in FM and AFM layers, careful structural characterization is essential. Figure 2(a) shows the XRD profiles for samples S1, S3, and S4. The unlabeled peaks are from the MgO(001) single-crystal substrate. For $FePt_{Oop}$/NiO bilayers, apart from the NiO and MgO peaks from the NiO spacer and the substrate, only the FePt 001 and FePt 002 peaks are observable, suggesting a strong FePt(001) texture. The appearance of the FePt 001 superlattice peak indicates the ordering of the FePt layer and the degree of order calculated from XRD results is 0.52. Correspondingly, the FePt 001 and FePt 002 peaks observed in $FePt_{Oop}$/NiO/$FePt_{Ip}$ trilayers (S4) are from the bottom $L1_0$-ordered FePt layer. Note that the (001) textured $L1_0$-FePt film possesses a strong perpendicular magnetic anisotropy, leading to the magnetization of the bottom FePt layer along the film normal direction. In the case of $FePt_{Ip}$/NiO/$FePt_{Ip}$ trilayers, the absence of the 001 and the relatively low angle 002 FePt peak indicate that the top FePt layer remains disordered. As mentioned above, the structural properties of NiO play a crucial role in determining the configuration of FM-AFM interfacial coupling. Thus, it is important to obtain the designed structure of the NiO spacer. Compared with bilayers, it is surprising that for both trilayers the split of the NiO 111 peak appears, which could be attributed to the sandwiched and upper protective NiO layers. Taking the FePt/NiO bilayers as a reference, the low-angle 111 peak corresponds to the sandwiched NiO spacer. The nearly same 2θ position indicates that the sandwiched NiO spacer experiences almost same strain as that in bilayers, and this strain as reported from our previous work [24] will be an in-plane anisotropic strain. On the other hand, an out-of-plane compressive strain could result in the XRD peak shift to a high-angle site. The peak shift of the NiO protective layer indicates a compressive strain in the film normal direction. Since the natural exchange striction leads to a compressive strain along the $\langle 111 \rangle$ direction [26], the NiO protective layer should favor a [111] stacking direction. Consequently, the NiO easy plane will be coplanar with the (111) interface, possessing a fairly low in-plane anisotropy [25]. In consideration of low in-plane anisotropy and free upper surface, the influence of the protective NiO layer on the adjacent FePt layer should be negligible small. Moreover, besides all the peaks discussed above, an additional FePt 111 peak can also be observed in both trilayers. It seems that other than the bottom FePt layer, the top FePt follows the same crystallographic orientation with the sandwiched NiO spacer, i.e., the (111) texture for the upper FePt layer.

To understand the in-plane orientations of the two FePt layers in the $FePt_{Oop}$/NiO/$FePt_{Ip}$ trilayer structure, the XRD 180° φ scans were carried out. The φ-scan plots for the {113} family of $FePt_{Oop}$ and the {113} family of $FePt_{Ip}$ are shown in Fig. 2(b). It is seen that two symmetrical peaks from the $FePt_{Oop}$ {113} reflections are located at same φ angle as the MgO {113} reflections, suggesting the bottom FePt layer well epitaxially grown on the MgO(001) substrate. Due to the weak signal from the NiO spacer, the in-plane orientations of NiO could not be obtained by φ scans. However, from our pervious study on FePt/NiO bilayers [24], it was shown that the NiO($\bar{1}\,\bar{1}\,1$) layer exhibits an in-plane 12-fold symmetry [the inset of Fig. 2(b)] and the growth relationship between FePt and NiO is determined as FePt(001) // NiO($\bar{1}\,\bar{1}\,1$); FePt[$1\bar{1}0$] // NiO[$1\bar{1}0$]. For such epitaxial relationship, an in-plane anisotropic strain will be induced, giving rise to a [$\bar{1}\,\bar{1}\,1$] NiO stacking direction. As a consequence, the Fe and Ni spins should be orthogonally coupled. As shown in the top panel of Fig. 2(b), the $A1$-disordered FePt layer exhibits 6 peaks with an azimuthal interval of 30°, indicating in plane 12-fold symmetry. These results show that the top FePt layer follows the same epitaxial relationship as the NiO spacer. Finally, the entire epitaxial relationship in the $FePt_{Oop}$/NiO/$FePt_{Ip}$ trilayer structure is established as follows: MgO(001) // $FePt_{Oop}$(001) // NiO($\bar{1}\,\bar{1}\,1$) // $FePt_{Ip}$($\bar{1}\,\bar{1}\,1$); MgO[$1\bar{1}0$] // FePt[$1\bar{1}0$] // NiO[$1\bar{1}0$] // FePt[$1\bar{1}0$].

B. Induced in-plane anisotropy of the $A1$-disordered FePt layer in $FePt_{Oop}$/NiO/$FePt_{Ip}$ trilayers through field cooling

On the basis of the 90° spin configuration between the two FM layers in the $FePt_{Oop}$/NiO/$FePt_{Ip}$ trilayers, the influence of the AFM spin alignment of NiO on the

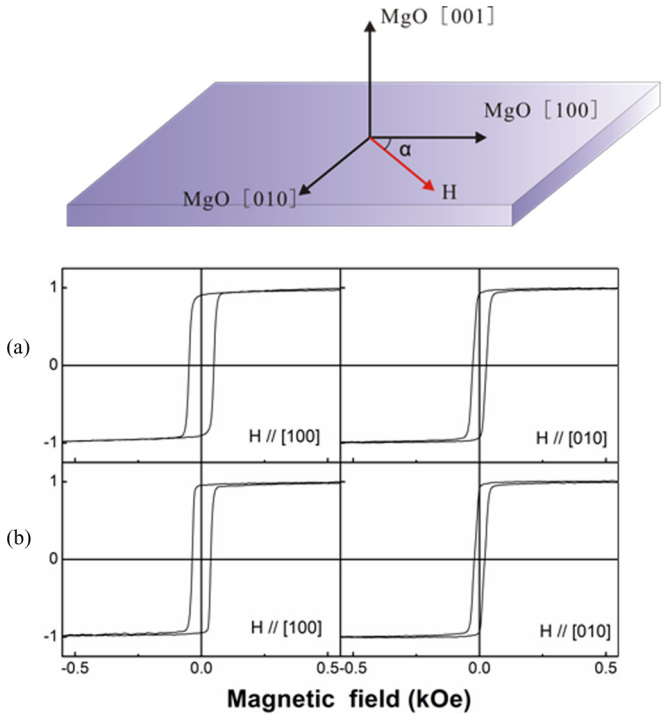

FIG. 3. In-plane hysteresis loops of $FePt_{Ip}$(3.5 nm)/NiO(4 nm)/$FePt_{Ip}$(3.5 nm) (S4) trilayers (a) before, and (b) after in-plane FC. The FC was performed with the external field along the MgO [100] axis and measurements were conducted with the field along the bottom FePt layer [100] and [010] axes, respectively. The inset shows the measurement geometry, in which the angle α denotes the angle between magnetic field and the MgO [100] axis in the film plane.

in-plane anisotropy of the top $A1$-disordered FePt has been subsequently studied. Figure 3(a) shows the in-plane hysteresis loops of $FePt_{Ip}$/NiO/$FePt_{Ip}$ trilayers. The magnetic field was applied along the MgO [100] and [010] axes, respectively. It is worth mentioning that the fcc CoPt possesses a cubic magnetocrystalline anisotropy with the easy axis along the $\langle 111 \rangle$ directions and its value [27] is $K_{mc} \sim 6 \times 10^5$ ergs/cm^3; a similar value is expected in the case of disordered FePt [28]. The typical square easy axis loops with nearly the same remanent magnetization are observed in two orthogonal measuring directions, indicating that both the bottom FePt(001) and top FePt(111) layer possess magnetic isotropy along these two directions. It is well accepted that the FC treatment could modify the AFM spin structure [19]. The experimental evidence shows that, for MgO(001)/CoO/Fe bilayers, in-plane uniaxial magnetic anisotropy in the Fe layer can be induced by FC treatment [12,29]. However, due to the weak NiO anisotropy in the $(\bar{1}\,\bar{1}\,1)$ plane [25,30], there is no significant change to the hysteresis loop after in-plane FC with the field along the MgO [100] axis, especially for the remanent magnetization as shown in Fig. 3(b). The almost 100% remanent magnetization in both hysteresis loops strongly suggests that at two FePt/NiO interfaces, the FM-AFM coupling should be of the same type, i.e., either collinear or orthogonal coupling. Since the layer thickness of the NiO spacer is thinner than 6 nm, no exchange bias exists in this work [31]. Besides, among hysteresis loops in Fig. 3(a) the slight coercive field differences may also be concerned. Generally, in FM/AFM bilayers the enhancement of coercive field can be understood as originating from coupling at the FM/AFM interface with rotatable AFM spins [32]. The winding and unwinding of the AFM NiO domain walls [10] during the FePt magnetic switching process may account for these differences, but the discussion is beyond the scope of this work.

To investigate the influence of the NiO spacer on the hysteresis behavior of the FePt layer in FM/AFM/FM trilayers, a particular case is the structure with 90° spin alignment configuration between the two FM layers as mentioned above. In $FePt_{Oop}$/NiO/$FePt_{Ip}$ trilayers, to distinguish the magnetization of the bottom and top FePt layers from the hysteresis loop measurement, a relatively small magnetic field of 850 Oe was applied to saturate the top $A1$-disordered FePt layer, whereas the magnetization contribution from bottom $L1_0$-ordered FePt layer is fairly small because of the strong perpendicular magnetic anisotropy. By using this approach, the in-plane hysteresis loops of the top FePt layer can be obtained as shown in Fig. 4. For as-grown trilayers, along both in-plane directions of measurement, the hysteresis loops exhibit a remanent magnetization of almost 100% with same coercive field in Fig. 4(a). After FC with the field along the MgO [100] axis, a different hysteresis behavior appears, which is not observed in the case of $FePt_{Ip}$/NiO/$FePt_{Ip}$ trilayers. For the magnetic field along the MgO [100] axis, the remanent

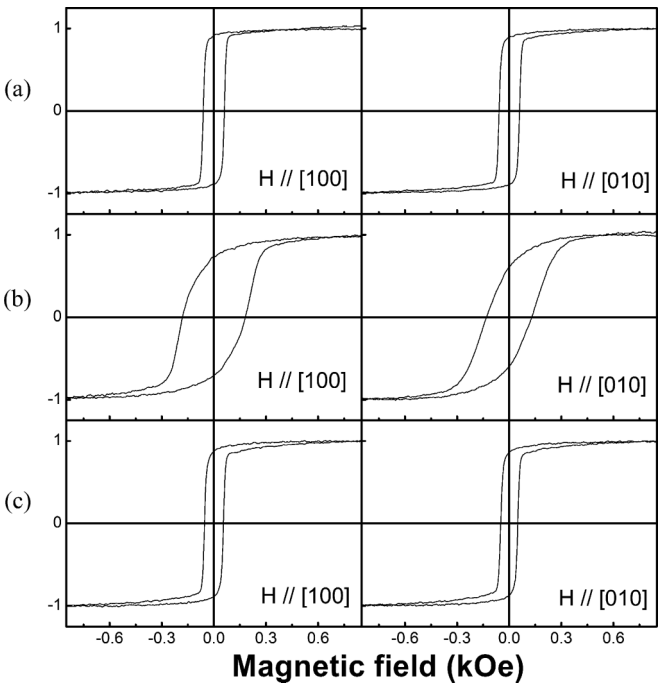

FIG. 4. In-plane hysteresis loops of the top $A1$-disordered FePt layer in $FePt_{Oop}$(4.5 nm)/NiO(4 nm)/$FePt_{Ip}$(3.5 nm) (S3) trilayers (a) before, (b) after in-plane FC with the field along the MgO [100] axis, and (c) subsequent out-of-plane FC with the field along the MgO [001] axis. The measurements were conducted with the field along the MgO [100] and [010] axes, respectively. In this small magnetic field range, due to the strong perpendicular magnetic anisotropy, the magnetization contribution from the bottom ordered FePt layer is negligible.

magnetization is reduced to 72% with enlarged coercive field of 182 Oe, while for its orthogonal direction, an even smaller remanent magnetization of 60% and a reduced coercive field of 130 Oe are observed as shown in Fig. 4(b). These results show clearly that the modification of AFM spin structure through in-plane FC induces in-plane magnetic anisotropy in the $A1$-disordered FePt layer. By subsequently performing an out-of-plane FC, the hysteresis loops for both two directions recover to the square easy axis loops as shown in Fig. 4(c), which are the same as the loops of the as-grown top FePt layer. Since the FM/AFM interface conditions including roughness and defects determine the types of interfacial coupling [33,34], the recovery of hysteresis loops after out-of-plane FC indicates that the heating process during FC will not give a significant consequence on the FM/AFM interface; namely, it will not affect the FM-AFM interfacial coupling. To clarify the mechanism of this induced in-plane anisotropy in Fig. 4(b), the configuration of the FM-AFM interfacial coupling must be understood. Based on careful structural characterization and previously reported work [24,35], the in-plane anisotropic strain in NiO should lead to the out-of-plane [$\bar{1}\ \bar{1}\ 1$] stacking direction being favorable, forming a compensated AFM interface. Since the AFM spins are antiparallel to each other at the compensated interface, the FM spins rotate in order to form an energetically favorable FM-AFM coupling configuration. As a result, the Fe spins in the top and bottom FePt layers are perpendicular to the Ni spins, lying in the film plane and film normal plane, respectively. However, in such coupling configuration, if the angle between FM and AFM spins is exactly 90°, the out-of-plane magnetization of Fe in the bottom FePt layer has no effect on the in-plane anisotropy of the top FePt layer. This is understood as the bottom FePt layer not being able to provide extra pinning for the in-plane rotation of Ni spins. Thus, results similar to those in Fig. 3(b) should be expected.

From our previous work, we have shown experimental evidence that at the compensated AFM interface for the spin-flop coupling configuration the angle between FM and AFM spins may not be exactly 90° [24]. In fact, such spin flop has already been predicted from theoretical calculation. A more detailed description is that at the fully compensated AFM interface, the competing interfacial and antiferromagnetic energy results in the AFM spins deviate slightly from its easy axis to generate a net magnetic moment. Consequently,

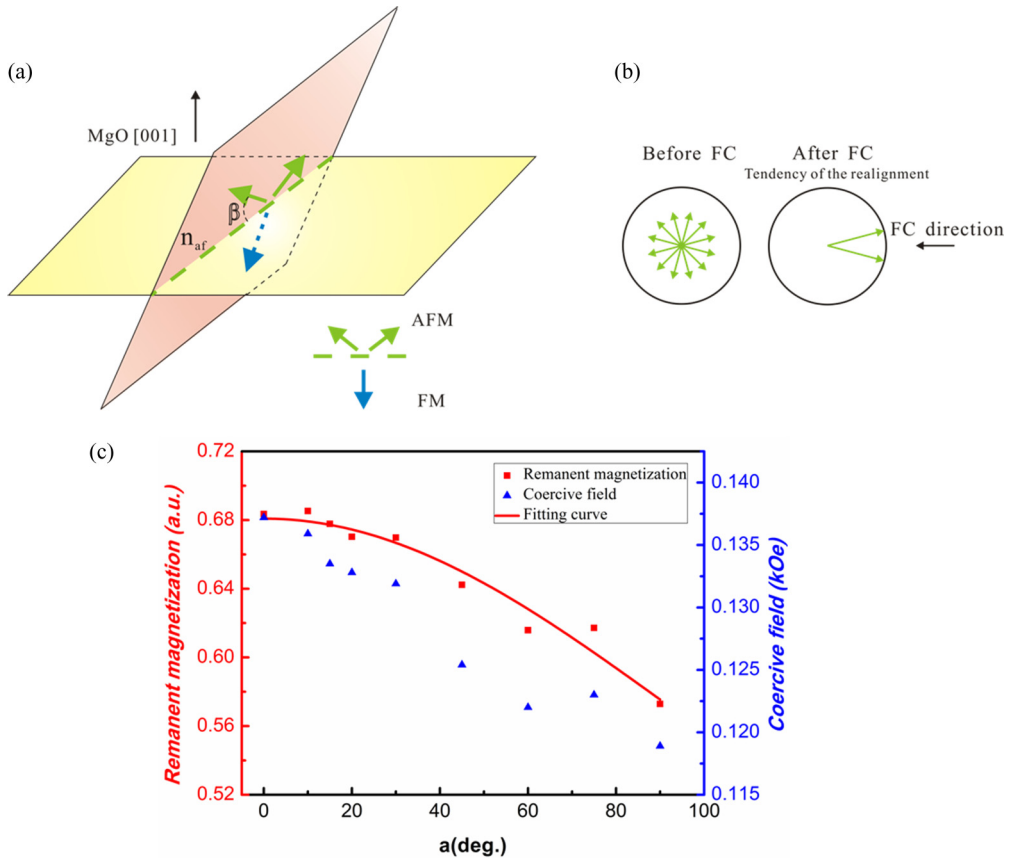

FIG. 5. (a) Schematic drawing of spins canting in the $FePt_{Oop}(001)/NiO(\bar{1}\ \bar{1}\ 1)$ bilayers; the dashed blue and green arrows correspond to the FM and AFM spins, respectively. Nonzero β presents the small deviation angle of Ni spins away from the ($\bar{1}\ \bar{1}\ 1$) easy plane. The inset shows the spin-flop coupling configuration, where the deviation of the FM-AFM coupling angle from 90° is somewhat exaggerated. (b) The proposed in-plane projection of the net magnetic moment generated from the AFM spin canting before and after in-plane FC. After FC, the in-plane components tend to be along the two easy axes, which are close to the direction of the field during FC. (c) The remanent magnetization (square symbol) and coercive field (triangle symbol) versus measuring angle α for top $A1$-disordered FePt layer in $FePt_{Oop}$(4.5 nm)/NiO(2 nm)/$FePt_{Ip}$(3.5 nm) (S2) trilayers. α denotes the angle between the measurement direction and the direction of the field during in-plane FC (MgO [100] direction).

the FM spin aligns antiparallel to this induced moment, orienting perpendicular to AFM easy axis as shown in the inset of Fig. 5(a) [6–8]. For $FePt_{Oop}$/NiO bilayers, due to this spin-flop coupling, the out-of-plane magnetization of Fe leads to a slightly slanted Ni spin at the interface off the $(\bar{1}\,\bar{1}\,1)$ easy plane as shown in Fig. 5(a) (green arrows) [24]. Correspondingly, the Fe magnetization will also deviate slightly from the film normal direction. Following the idea of FM and AFM spin alignment in the spin-flop coupling configuration as given above, it will provide an extra pinning effect on the in-plane rotation of AFM spins around the axis perpendicular to the film plane, because of the spins canted off the $(\bar{1}\,\bar{1}\,1)$ easy plane that has relative high anisotropy energy [36]. For $FePt_{Oop}$/NiO/$FePt_{Ip}$ trilayers, it is reasonable to assume the same FM-AFM coupling configuration as in $FePt_{Oop}$/NiO bilayers. In this case, the in-plane FC may enhance the coupling at the NiO/$FePt_{Ip}$ interface, canting the AFM spins to be closer to the $(\bar{1}\,\bar{1}\,1)$ NiO plane. As a result, the increased in-plane component of Ni spins and the extra pinning provided by the out-of-plane aligned Fe spins will make the rotation of in-plane Fe spins difficult in the top $A1$-disordered FePt layer. This effect cannot be expected by the exact 90° FM-AFM coupling configuration.

To further understand the FC-induced in-plane anisotropy in the top FePt layer, we investigated the angular dependence of the remanent magnetization of the top FePt layer, as shown in Fig. 5(c). Here, α refers to the angle between the direction of the measurement and the applied field during in-plane FC. In order to enhance the pinning from the bottom FePt layer and avoid the formation of a spiral domain wall in NiO, we decreased the NiO spacer thickness to 2 nm. It is known that the magnetic ordering temperature of AFM thin films strongly decreases as the film thickness decreases [37,38]. In the case of the NiO thin film, the Néel temperature going from 520 K for the bulk to 295 K for a 5 monolayer film has been reported [39]. Therefore, the NiO spacer of 2 nm used in this work should keep the AFM order at RT. In addition, the measurement sequence was randomly arranged to eliminate the contribution from a possible training effect. As seen in Fig. 5(c), with increasing angle α, both remanent magnetization and coercive field show a strong tendency to decrease, indicating the in-plane anisotropy of top FePt layer. Then the data were quantitatively analyzed. For the spin-flop coupling configuration, as explained in last paragraph, the induced in-plane anisotropy in the top FePt layer is mainly related to the projection of net magnetic moment generated from AFM spins. In the following, we will focus on this in-plane component. Since the growth structure of the NiO spacer shows 12-fold symmetry around the film normal direction, 12 equivalent in-plane components of the AFM net moment can be expected, which are generated by the spin canting. Such magnetization components are perpendicular to one of six easy axes in the NiO$(\bar{1}\,\bar{1}\,1)$ plane. The idea is that the in-plane FC could induce a modification of Ni spin structure [21], leading to those 12 components tending to be along two directions (stable contribution), which are close to the direction of the field during FC as shown in Fig. 5(b). Meanwhile, the enhanced coupling at the upper interface results in an increase of the in-plane component of Ni spin as discussed above. Due to the thermal fluctuation at RT, in other words, unstable AFM order, another contribution from randomly distributed in-plane components (unstable contribution) should also exist. This contribution resembles the case of uniaxial FM film with its easy axis randomly distributed in the film plane. Based on this idea, the remanent magnetization of the top FePt layer should follow the expression

$$I_r = \frac{2b}{\pi}\int_0^{\frac{\pi}{2}} I_s \cos\alpha d\alpha + \frac{c}{2} I_s\left[\cos\left(\alpha - \frac{\pi}{6}\right) + \cos\left(\alpha + \frac{\pi}{6}\right)\right], \quad (1)$$

where I_r and I_s are the remanent magnetization and saturation magnetization, respectively; α denotes the angle between the direction of the measurement and the field during in-plane FC; b and c are the portions of stable and unstable contributions, respectively. By fitting the data in Fig. 5(c) (square symbol), the b and c values obtained from data fitting are 90% and 11%, respectively. As shown in Fig. 5(c), Eq. (1) well fits the experimental data, which exhibit a clear angular dependence with respect to the measuring direction. Then, we conclude that the roles of the in-plane field on the NiO spin structure are the enhancement of coupling at the upper interface and realignment of the Ni spin in-plane component.

C. Stripe domain evolution of the $L1_0$-ordered FePt layer in $FePt_{Oop}$/NiO/$FePt_{Ip}$ trilayers after field cooling

The magnetic domain structure of $FePt_{Oop}$(4.5 nm)/NiO (4 nm) bilayers and $FePt_{Oop}$(4.5 nm)/NiO(4 nm)/$FePt_{Ip}$ (3.5 nm) trilayers was studied by magnetic force microscopy

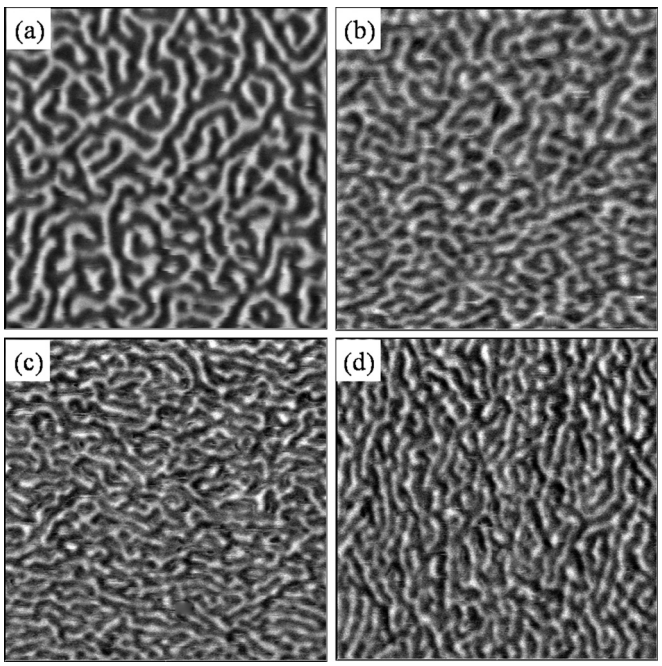

FIG. 6. Magnetic domain structure at remanence in (a) FeP t_{Oop}(4.5 nm)/NiO(4 nm) (S1) bilayers, (b) $FePt_{Oop}$(4.5 nm)/NiO (4 nm)/$FePt_{Ip}$(3.5 nm) (S3) trilayers. (c) Image of $FePt_{Oop}$ (4.5 nm)/NiO(4 nm)/$FePt_{Ip}$(3.5 nm) trilayers after in-plane FC. (d) Rotating the scanning direction of (c) around film normal direction by 90°. All images are 5 × 5 μm.

(MFM) at RT. For $FePt_{Oop}/NiO/FePt_{Ip}$ trilayers, the in-plane magnetization of the ultrathin top FePt layer generates a fairly weak stray field, which is hardly detected by the magnetized tip. Thus, it is reasonable to expect that the observed domain structures should be from the bottom FePt layer. As shown in Fig. 6(a), the $FePt_{Oop}/NiO$ bilayers exhibit stripe domain structure with random alignment. With the deposition of the top $A1$-disordered FePt layer, no significant change can be observed unless there is a minute reduction of the stripe width from approximately 147 nm to 134 nm [Fig. 6(b)]. To study the effect of the modification of AFM spin structure on the domain structure, we performed in-plane FC on the sample of S3. Note that the FC temperature (525 K) is well below the reported Curie temperature (700 K) of partially ordered FePt film [40]. Thus, the FC treatment itself should have no effect on domain structure of the bottom FePt layer. Figure 6(c) shows the domain structure of the bottom FePt layer in $FePt_{Oop}/NiO/FePt_{Ip}$ trilayers after in-plane FC. It is clearly seen that the stripes tend to be parallel to the direction of the field during FC. After rotating the scanning direction around the MgO [001] axis by 90°, the alignment of the stripe domain also changes its direction by 90°, which is a strong indication that the Fe magnetization slightly deviates from the film normal direction. Moreover, comparing with the as-grown $FePt_{Oop}/NiO/FePt_{Ip}$ trilayers, the stripe width reduces to an even smaller value (107 nm). Taking into account the FM-AFM spin-flop coupling configuration as mentioned above, the observed decrease of the stripe width can be well explained. For sample S3, the in-plane Fe magnetization in the top FePt layer aligns the AFM spin of NiO slightly closer to the film plane. Consequently, the in-plane component of the net magnetic moment generated from AFM spins will be enhanced. It is known that the reduced stripe domain width can be attributed to reduced perpendicular magnetic anisotropy [41]. Therefore, compared with the case of $FePt_{Oop}/NiO$ bilayers, the reduction of the stripe width in $FePt_{Oop}/NiO/FePt_{Ip}$ trilayers is not surprising. As discussed in the proceeding section, the in-plane FC could result in a further enhancement of the NiO spin in-plane component. This explains why the modification of the AFM spin structure in the NiO spacer through the in-plane FC could affect the stripe width in the bottom FePt layer.

IV. CONCLUSIONS

We have studied the structural and magnetic properties of the $FePt_{Oop}/NiO/FePt_{Ip}$ trilayer structure, where the bottom and top FePt layers are partially ordered and disordered, respectively. Magnetic hysteresis loop measurements show that the Fe magnetization in the top FePt layer is in the film plane, while that in bottom layer is perpendicular to the film plane. This feature gives rise to a 90° spin configuration between the two FM layers, regardless of the NiO spacer. The key point of this study is that by modifying the NiO spin structure through FC we modulate the magnetic performance of the two FM layers. For as-grown $FePt_{Oop}/NiO/FePt_{Ip}$ trilayers, the top FePt layer exhibits an in-plane "isotropy." However, after in-plane FC, we find that the remanent magnetization depends on the measuring angle relative to the direction of the field during in-plane FC, which is an indication of in-plane anisotropy. Realizing the effect on the top FePt layer, the bottom FePt layer was further studied by magnetic domain imaging. After in-plane FC, the stripe domain shows realignment and tends to be parallel to the direction of the applied field during FC, confirming the existence of small deviating angle of Fe magnetization from the film normal direction, while a reduction of stripe width can also be observed. In consideration of the FM-AFM interaction, the interesting results observed in this work can be well explained by the spin-flop coupling configuration, in which the angle between the FM and AFM spins is not exactly 90°. Furthermore, this study may provide a method to induce magnetic anisotropy in the FM/AFM/FM sandwiched structure.

ACKNOWLEDGMENT

This work was partially supported by JSPS Grant-in-Aid for Challenging Exploratory Research Grant No. JP16K14372.

[1] W. H. Meiklejohn and C. P. Bean, Phys. Rev. **102**, 1413 (1956).
[2] Shunsuke Fukami, Chaoliang Zhang, Samik DuttaGupta, Aleksandr Kurenkov, and Hideo Ohno, Nat. Mater. **15**, 535 (2016).
[3] Yong-Chang Lau, Davide Betto, Karsten Rode, J. M. D. Coey, and Plamen Stamenov, Nat. Nanotechnol. **11**, 758 (2016).
[4] D. Mauri, H. C. Siegmann, P. S. Bagus, and E. Kay, J. Appl. Phys. **62**, 3047 (1987).
[5] A. P. Malozemoff, Phys. Rev. B **35**, 3679 (1987).
[6] N. C. Koon, Phys. Rev. Lett. **78**, 4865 (1997).
[7] R. L. Stamps, J. Phys. D **33**, R247 (2000).
[8] M. D. Stiles and R. D. McMichael, Phys. Rev. B **59**, 3722 (1999).
[9] Wondong Kim, E. Jin, J. Wu, J. Park, E. Arenholz, A. Scholl, Chanyong Hwang, and Z. Q. Qiu, Phys. Rev. B **81**, 174416 (2010).
[10] J. Li, A. Tan, S. Ma, R. F. Yang, E. Arenholz, C. Hwang, and Z. Q. Qiu, Phys. Rev. Lett. **113**, 147207 (2014).
[11] J. Wu, J. S. Park, W. Kim, E. Arenholz, M. Liberati, A. Scholl, Y. Z. Wu, Chanyong Hwang, and Z. Q. Qiu, Phys. Rev. Lett. **104**, 217204 (2010).
[12] Q. Li, G. Chen, T. P. Ma, J. Zhu, A. T. N'Diaye, L. Sun, T. Gu, Y. Huo, J. H. Liang, R. W. Li, C. Won, H. F. Ding, Z. Q. Qiu, and Y. Z. Wu, Phys. Rev. B **91**, 134428 (2015).
[13] J. Li, Y. Meng, J. S. Park, C. A. Jenkins, E. Arenholz, A. Scholl, A. Tan, H. Son, H. W. Zhao, Chanyong Hwang, Y. Z. Wu, and Z. Q. Qiu, Phys. Rev. B **84**, 094447 (2011).
[14] Bo-Yao Wang, Jhen-Yong Hong, Kui-Hon Ou Yang, Yuet-Loy Chan, Der-Hsin Wei, Hong-Ji Lin, and Minn-Tsong Lin, Phys. Rev. Lett. **110**, 117203 (2013).
[15] A. Tan, J. Li, C. A. Jenkins, E. Arenholz, A. Scholl, C. Hwang, and Z. Q. Qiu, Phys. Rev. B **88**, 104404 (2013).
[16] J. S. Moodera, L. R. Kinder, T. M. Wong, and R. Meservey, Phys. Rev. Lett. **74**, 3273 (1995).

[17] Z. Y. Liu and S. Adenwalla, Phys. Rev. Lett. **91**, 037207 (2003).
[18] P. A. A. van der Heijden, C. H. W. Swüste, W. J. M. de Jonge, J. M. Gaines, J. T. W. M. van Eemeren, and K. M. Schep, Phys. Rev. Lett. **82**, 1020 (1999).
[19] J. Camarero, Y. Pennec, J. Vogel, M. Bonfim, S. Pizzini, F. Ernult, F. Fettar, F. Garcia, F. Lançon, L. Billard, B. Dieny, A. Tagliaferri, and N. B. Brookes, Phys. Rev. Lett. **91**, 027201 (2003).
[20] J. Wu, J. Choi, A. Scholl, A. Doran, E. Arenholz, Y. Z. Wu, C. Won, Chanyong Hwang, and Z. Q. Qiu, Phys. Rev. B **80**, 012409 (2009).
[21] W. Zhu, L. Seve, R. Sears, B. Sinkovic, and S. S. P. Parkin, Phys. Rev. Lett. **86**, 5389 (2001).
[22] H. Ohldag, A. Scholl, F. Nolting, S. Anders, F. U. Hillebrecht, and J. Stöhr, Phys. Rev. Lett. **86**, 2878 (2001).
[23] N. J. Gökemeijer, J. W. Cai, and C. L. Chien, Phys. Rev. B **60**, 3033 (1999).
[24] Tenghua Gao, Nobuhide Itokawa, Jian Wang, Youxing Yu, Takashi Harumoto, Yoshio Nakamura, and Ji Shi, Phys. Rev B **94**, 054412 (2016).
[25] I. P. Krug, F. U. Hillebrecht, M. W. Haverkort, A. Tanaka, L. H. Tjeng, H. Gomonay, A. Fraile-Rodríguez, F. Nolting, S. Cramm, and C. M. Schneider, Phys. Rev. B **78**, 064427 (2008).
[26] G. A. Slack, J. Appl. Phys. **31**, 1571 (1960).
[27] R. A. McCurrie and P. Gaunt, Philos. Mag. **13**, 567 (1966).
[28] E. Sallica Leva, R. C. Valente, F. Martínes Tabares, M. Vásquez Mansilla, S. Roshdestwensky, and A. Butera, Phys. Rev. B **82**, 144410 (2010).
[29] W. N. Cao, J. Li, G. Chen, J. Zhu, C. R. Hu, and Y. Z. Wu, Appl. Phys. Lett. **98**, 262506 (2011).
[30] C. H. Lai, T. Ming, R. Erwin, and J. Borchers, J. Appl. Phys. **91**, 7751 (2002).
[31] P. Luches, S. Benedetti, A. di Bona, and S. Valeri, Phys. Rev. B **81**, 054431 (2010).
[32] G. Scholten, K. D. Usadel, and U. Nowak, Phys. Rev. B **71**, 064413 (2005).
[33] J. Camarero. Y. Pennec, J. Vogel, S. Pizzini, M. Cartier, F. Fettar, F. Ernult, A. Tagliaferri, N. B. Brookes, and B. Dieny, Phys. Rev. B **67**, 020413(R) (2003).
[34] M. Finazzi, M. Portalupi, A. Brambilla, L. Duò, G. Ghiringhelli, F. Parmigiani, M. Zacchigna, M. Zangrando, and F. Ciccacci, Phys. Rev. B **69**, 014410 (2004).
[35] Anne D. Lamirand, Márcio M. Soares, Aline Y. Ramos, Hélio C. N. Tolentino, Maurizio De Santis, Julio C. Cezar, Abner de Siervo, and Matthieu Jamet, Phys. Rev. B **88**, 140401(R) (2013).
[36] M. T. Hutchings, Phys. Rev. B **6**, 3447 (1972).
[37] P. J. van der Zaag, Y. Ijiri, J. A. Borchers, L. F. Feiner, R. M. Wolf, J. M. Gaines, R. W. Erwin, and M. A. Verheijen, Phys. Rev. Lett. **84**, 6102 (2000).
[38] M. W. Haverkort, S. I. Csiszar, Z. Hu, S. Altieri, A. Tanaka, H. H. Hsieh, H.-J. Lin, C. T. Chen, T. Hibma, and L. H. Tjeng, Phys. Rev. B **69**, 020408 (2004).
[39] D. Alders, L. H. Tjeng, F. C. Voogt, T. Hibma, G. A. Sawatzky, C. T. Chen, J. Vogel, M. Sacchi, and S. Iacobucci, Phys. Rev. B **57**, 11623 (1998).
[40] S. Okamoto, N. Kikuchi, O. Kitakami, T. Miyazaki, Y. Shimada, and K. Fukamichi, Phys. Rev. B **66**, 024413 (2002).
[41] Y. Z. Wu, C. Won, A. Scholl, A. Doran, H. W. Zhao, X. F. Jin, and Z. Q. Qiu, Phys. Rev. Lett. **93**, 117205 (2004).